Polymer Journal (2018) 50:203–211
https://doi.org/10.1038/s41428-017-0004-8

ORIGINAL ARTICLE

A facile method for the controlled polymerization of biocompatible and thermoresponsive oligo(ethylene glycol) methyl ether methacrylate copolymers

Teresa Alejo[1,2] · Martín Prieto[1,2] · Hugo García-Juan[3] · Vanesa Andreu[1,2] · Gracia Mendoza[1,2] · Víctor Sebastián[1,2,4] · Manuel Arruebo[1,2,4]

Received: 18 July 2017 / Revised: 18 September 2017 / Accepted: 10 October 2017 / Published online: 9 January 2018
© The Society of Polymer Science, Japan 2018

Abstract

Photochemically controlled ATRP-like polymerization is successfully used to prepare a thermoresponsive copolymer of oligo(ethylene glycol) methyl ether methacrylate (OEGMA) and di(ethylene glycol) methyl ether methacrylate (MEO_2MA). The photochemically controlled method described here provides good control over the polymer structure, architecture, and properties. This photopolymerization renders polymers with narrow molecular weight distributions (Mw/Mn = 1.3) and high monomer conversions (>90%) while using a very low iridium-based catalyst concentration (25 ppm). In addition, the reaction rate of this polymerization is fast, reaching 50% monomer conversion in less than 1 h of reaction. The lower critical solution temperature (LCST) of the prepared polymer was also adjusted to be in the range of physiological temperatures, undergoing a coil-to-globule transition at 43 °C. In addition, the resulting polymer showed no cytotoxicity on four mammalian cell lines at the highest concentration tested (0.4 mg/ml), which highlights its potential use in different biomedical applications.

Introduction

Stimuli responsive copolymers derived from oligo(ethylene glycol) methacrylate are promising biocompatible materials that present thermoresponsive properties, making them suitable as injectable drug delivery systems [1–3]. Common thermosensitive polymers, such as poly(N-isopropylacrylamide) (PNIPAM), have been used in different biomedical applications, including triggered drug delivery [4], biosensing [5], cell culturing [6], encapsulation [7], and tissue engineering [8]. However, PNIPAM presents some disadvantages, such as low biocompatibility and hysteresis in its phase transition, compared to oligo(ethylene glycol) methyl ether methacrylate (OEGMA)-based copolymers [9, 10]. The PNIPAM cytotoxicity has been reported to depend on the concentration of leftover monomer, deposition method (when supported on a substrate), studied cell line, and presence of impurities [11]. Both PNIPAM- and OEGMA-based copolymers are soluble in water and undergo a transition to water-insoluble materials at a certain temperature called the lower critical solution temperature (LCST). This transition temperature can be influenced by structural parameters, such as the architecture [12], hydrophobic content [13], and molecular weight of the polymer [14], and it can be tuned by changing the OEGMA and di(ethylene glycol) methyl ether methacrylate (MEO_2MA) monomer ratio [15].

In the past decade, OEGMA-based polymers have been successfully synthesized using different free-radical

Teresa Alejo and Martin Prieto contributed equally to this work.

Electronic supplementary material The online version of this article (https://doi.org/10.1038/s41428-017-0004-8) contains supplementary material, which is available to authorized users.

✉ Teresa Alejo
teresaal@unizar.es

[1] Department of Chemical Engineering, Aragón Institute of Nanoscience (INA), University of Zaragoza, Campus Río Ebro-Edificio I+D, C/Poeta Mariano Esquillor S/N, 50018 Zaragoza, Spain

[2] Aragon Health Research Institute (IIS Aragón), 50009 Zaragoza, Spain

[3] Departamento de Química Orgánica, Facultad de Ciencias, Instituto de Ciencia de Materiales de Aragón (ICMA), Universidad de Zaragoza-CSIC, 50009 Zaragoza, Spain

[4] Networking Research Center on Bioengineering, Biomaterials and Nanomedicine, CIBER-BBN, 28029 Madrid, Spain

polymerization methods, such as atom transfer radical polymerization (ATRP) [16, 17] and reversible addition-fragmentation chain transfer polymerization (RAFT) [18, 19]. Nevertheless, RAFT polymerizations present some limitations; first, it is necessary to choose a suitable RAFT agent for the preparation of well-defined polymers, and typically, the design of a RAFT agent involves multiple synthetic steps and subsequent purifications of complex organic compounds [20]. Another drawback is that the RAFT agents can suffer degradation over time, producing sulfur compounds that might be adverse in some applications [21]. For instance, Boyer et al. [22] reported the copolymerization of oligo(ethylene glycol) acrylate and di(ethylene glycol) acrylate monomers in acetonitrile at 60 °C to produce thermoresponsive copolymers with a dispersity below 1.3 after 5 h; however, a non-commercial RAFT agent, 3-(benzylsulfanylthiocarbonylsulfanyl) propionic acid (BSPA), was necessary.

Lutz et al. [15] reported the preparation of thermoresponsive copolymers based on OEGMA using ATRP. They reported the ATRP of OEGMA and MEO_2MA copolymers initiated by methyl 2-bromopropionate (MBP) using a chloride-based CuCl/bipy catalyst in ethanol at 60 °C, with a dispersity of 1.27 and monomer conversions of 90–95% after 9–10 h of reaction, which led to much better control over the polymerization than the use of bromide-based catalysts. However, ATRP typically employs a molar ratio of monomer to copper (used as the catalyst) of 100:1. Because of the high amounts of catalyst employed in those ATRP procedures, the polymers must be exhaustively purified after reaction, resulting in high economic and environmental costs. Moreover, conventional ATRP reactions are usually carried out at high temperatures as well as with long reaction times, which are required to reach acceptable reaction yields [23–25]. ATRP is not applicable with the polymerization of some monomeric species, such as acidic monomers, due to their interactions with ligands producing carboxylate salts. Other monomers, such as vinyl esters, halogenated alkenes and alkyl-substituted olefins, are hardy polymerized by ATRP due to their low reactivities in radical polymerizations that usually have very low equilibrium constants [23]. Most typical Cu-mediated radical polymerizations present some drawbacks, such as high sensitivity of the catalyst to oxygen and water and the requirement of exhaustive polymer purification processes to remove traces of potentially toxic metals. The development of efficient and facile strategies for the synthesis of well-defined polymer architectures using ultralow catalyst concentrations is a significant challenge necessary to overcome. Regarding this issue, using initiators for continuous activator regeneration atom transfer radical polymerization (ICAR ATRP) was proposed as a promising technique to synthesize well-defined polymers using very low catalyst concentrations (<50 ppm) [26]. In this strategy, thermoresponsive OEGMA-based copolymers have been successfully prepared through copper-based ICAR ATRP with excellent control over the molecular weight and low dispersity (PDI = 1.15–1.28). However, slow polymerization rates have been observed, and in the best cases, 7 h of reaction were needed to reach conversions higher than 90% [27]. The synthesis of poly(methyl methacrylates) has been previously reported with a 99% monomer conversion after 6 h using photo-induced ATRP with ethyl bromoisobutyrate (EBiB) and copper(II) bromide ($CuBr_2$)/tris[2-(dimethylamino)ethyl]amine (Me_6-Tren) as catalysts under exposure to UV light [28]. It should be noted that some initiators are too active to use with copper-based catalysts and might lead to an excess of termination reactions rendering high dispersity [29]. Here, to compare the reported photopolymerizations, we used the same initiator, monomers, and solvent as the traditional standard protocol of OEGMA-based thermoresponsive polymers establish by Lutz et al. [15]. Photochemical-controlled ATRP-like polymerization is a versatile and efficient method for rendering well-defined architectures over a wide range of monomers, including homopolymers and block copolymers of methacrylates, styrene, N-vinylpyrrolidinone, and others [30–36]. In this regard, Fors et al. [30] developed, for the first time, a controlled/living radical polymerization of methacrylate activated by light using a photoredox iridium-based catalyst. In the present work, P(MEO_2MA-co-$OEGMA_{500}$) copolymers were prepared through a photochemically controlled ATRP-like polymerization using an $Ir(ppy)_3$ catalyst to activate the polymerization under UV light. This technique presents several further advantages compared to conventional ATRP-based methods. The photopolymerization can be performed at room temperature using a reduced amount of catalyst (i.e., in the ppm range) and renders very well-controlled polymer architectures. In this work, we compared the conventional ATRP synthesis with the here-described photo-induced polymerization under the same reaction conditions. Different variables, such as the obtained polymer structures, architectures, dispersities, and molecular weight distributions, were analyzed. The photopolymerization showed fast polymerization kinetics and rendered well-defined polymers with narrow molecular weight distributions.

Experimental section

Materials and methods

MEO_2MA (Sigma-Aldrich, Madrid, Spain, 95%), OEGMA (Sigma-Aldrich, Madrid, Spain, Mn 500 g/mol), 2,2′-bipyridyl (bipy) (Sigma-Aldrich, Madrid, Spain, 98%),

methyl 2-bromopropionate (MBP) (Sigma-Aldrich, Madrid, Spain, 98%), tris[2-phenylpyridinato-C^2,N]iridium(III) ($Ir(ppy)_3$) (Sigma-Aldrich, Madrid, Spain, 99%), and anhydrous ethanol (Panreac Quimica SA, Barcelona, Spain, 0.02% water) were used as received. Copper(I) chloride (Sigma-Aldrich, Madrid, Spain, 97%) was washed with glacial acetic acid and ethanol and dried to remove oxidized species before use.

Gel permeation chromatography (GPC) was performed using tetrahydrofuran (THF) as the eluent at a flow rate of 1 ml/min. The GPC system was a Waters e2695 Alliance liquid chromatography system comprising two Ultra Styragel® columns (HR4 and HR2) with pore sizes of 500 and 10^4 Mw from Waters (Cerdanyola del Vallès, Spain) and a Waters 2424 evaporation light scattering detector. The system was calibrated with poly(methyl methacrylate) PMMA standards.

Proton nuclear magnetic resonance (^{1}H NMR) spectroscopy was carried out on a Bruker AV-400 spectrometer (Bruker BioSpin GmbH, Rheinstetten, Germany) operating at 400 MHz using $CDCl_3$ as the solvent.

The cloud points of the polymer solutions (3 mg/ml) in deionized water were obtained from optical transmittance measurements at 670 nm as a function of temperature using a Varian Cary® 50 UV-Visible spectrometer (Agilent Technologies, Santa Clara, USA) equipped with a fiber optic dip probe. The lower critical solution temperature (LCST) of the polymer was defined as the temperature at which 50% of the transmittance was reached [37].

Fourier transform infrared (FTIR) spectroscopy analysis was performed on a Bruker Vertex 70 FTIR spectrometer (Bruker BioSpin GmbH, Rheinstetten, Germany) equipped with a deuterated triglycine sulfate (DTGS) detector and a Golden Gate diamond attenuated total reflectance (ATR) accessory. The scans were performed in the wavelength range of 4000–400 per cm.

Synthetic procedures

Atom transfer radical polymerization (ATRP)

Thermoresponsive P(MEO_2MA-co-$OEGMA_{500}$) polymers were prepared by ATRP using a CuCl/bipy complex as the catalyst. The synthesis was performed in ethanol at 60 °C using a methyl 2-bromopropionate (MBP) initiator according to the method reported by Lutz and Hoth [15]. The polymerization conditions were $[monomers]_0/[MBP]_0/[CuCl]_0/[bipy]_0 = 100/1/1/2$ (molar ratio). Samples were taken throughout the reaction for ^{1}H NMR analysis to study the polymerization kinetics. The final product was purified by passing the ethanol solution through a silica gel (60–120 mesh) column. Then, the solvent was further removed using a rotary evaporator, and the polymer was dispersed in water and dialyzed (molecular weight cutoff 14,000 Da) against water/ethanol mixtures for at least 72 h to ensure the removal of the non-reacted monomers.

Photochemical-controlled ATRP-like polymerization

The photopolymerization was performed using a tris[2-phenylpyridinato-C^2,N]iridium (III) ($Ir(ppy)_3$) photocatalyst, activated upon UV irradiation with two light-emitting diodes (LEDs) with a 365 nm wavelength (radiant flux ~4.6 W) (see Supplementary Fig. S1). The reaction was performed in ethanol under stirring at room temperature using the ATRP initiator MBP. The reactions were performed using a molar ratio of $[monomers]_0/[MBP]_0/[Ir(ppy)]_0 = 100/1/2.5 \times 10^{-3}$. The photopolymerization reaction setup is described in the supporting information section.

Cell culture

Human dermal fibroblasts (Lonza, Belgium) and U251 MG glioblastoma (kindly gifted by Dr Pilar Martin-Duque) cell lines were grown using Dulbecco's modified Eagle's medium high glucose (DMEM with stable glutamine, Biowest) in a humidified atmosphere containing 5% CO_2 at 37 °C. The growth medium was supplemented with fetal bovine serum (FBS, 10% (v/v); Thermo Fisher Scientific) and antibiotic-antimycotic solution (60 µg/ml penicillin, 100 µg/ml streptomycin, and 0.25 µg/ml amphotericin B, Biowest).

The human acute monocytic leukemia suspension cell line (THP-1) was purchased from American Type Culture Collection (ATCC, TIB-202™; Manassas, VA, USA). The cells were cultured in RPMI 1640 medium (Gibco, Thermo Fisher Scientific) supplemented with fetal bovine serum (FBS, 10% (v/v); Thermo Fisher Scientific), non-essential amino acids (1%; Biowest), sodium pyruvate (1 mM; Biowest), HEPES (10 mM; Biowest), 2-mercaptoethanol (0.05 mM, Gibco, Thermo Fisher Scientific), stable glutamine (2 mM; Biowest), and antibiotic-antimycotic solution (60 µg/ml penicillin, 100 µg/ml streptomycin, and 0.25 µg/ml amphotericin B, Biowest) at 37 °C in a 5% CO_2 humidified incubator. Monocytic cells were differentiated into the adherent macrophage-like state in supplemented RPMI 1640 medium containing 1 µM phorbol 12-myristate 13-acetate (PMA, Sigma-Aldrich) for 72 h.

Mouse mesenchymal stem cells (mMSCs) were also kindly gifted by Dr Pilar Martin-Duque. This cell line was cultured in Dulbecco's modified Eagle's F-12 medium (DMEM F-12, Biowest) supplemented with fetal bovine serum (FBS, 10% (v/v); Thermo Fisher Scientific), stable glutamine (2 mM; Biowest), and antibiotic-antimycotic solution (60 µg/ml penicillin, 100 µg/ml streptomycin, and 0.25 µg/ml amphotericin B, Biowest) and maintained at 37 °

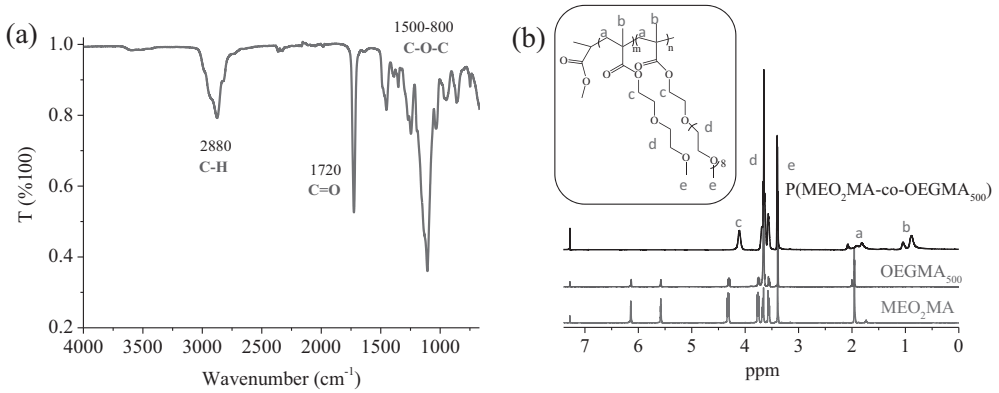

Fig. 1 **a** FTIR spectrum of the P(MEO_2MA-co-$OEGMA_{500}$) copolymer and **b** ^{1}H NMR spectra of the P(MEO_2MA-co-$OEGMA_{500}$) copolymer and $OEGMA_{500}$ and MEO_2MA monomers

C in a 5% CO_2 humidified atmosphere under hypoxic conditions (3% O_2).

Cell viability assay

In vitro cytotoxicity of the P(MEO_2MA-co-$OEGMA_{500}$) copolymer was evaluated using the Blue Cell Viability assay (Abnova) according to the manufacturer's instructions. U251 MG, fibroblasts, and mMSCs (densities of 5000, 6000, and 5000 cells/well, respectively) were seeded in a 96-well plate 24 h prior to incubation with P(MEO_2MA-co-$OEGMA_{500}$) and allowed to adhere. For differentiating the THP-1 monocytes into macrophages, THP-1 monocytes were seeded at a density of 70,000 cells/well in 96-well plates and differentiated with phorbol 12-myristate 13-acetate (PMA) for 3 days.

P(MEO_2MA-co-$OEGMA_{500}$) was added to the cells in complete growth medium at a concentration range of 0.025–0.4 mg/ml, and then, the cells were maintained in the standard culture conditions for 24 h. After incubation, the cells were washed with Dulbecco's phosphate-buffered saline (DPBS, Biowest) and incubated with complete growth medium containing 10% (v/v) CellQuanti-Blue reagent for 4 h. The fluorescence intensity of the medium was measured in a multi-mode Synergy HT Microplate Reader at excitation and emission wavelengths of 530 and 590 nm, respectively (Biotek). Cell viability was expressed as a relative percentage to the value of the untreated control cells. The percentages obtained depict the average of five values.

Results and discussion

Photochemically controlled living radical polymerizations of OEGMA and MEO_2MA monomers were investigated using an $Ir(ppy)_3$ complex as a catalyst under UV LED light ($\lambda_{max} = 365$ nm, 4.8 W, current 1A) used as an irradiation source. The iridium complex is characterized by a maximum absorption wavelength in the UV range (~370 nm). To obtain efficient light absorption, the reaction was irradiated near the maximum absorption wavelength of the iridium complex using a 365 nm LED. The reactions were carried out at room temperature in a Schlenk tube, where the OEGMA and MEO_2MA monomers were mixed with the MBP initiator in the presence of the $Ir(ppy)_3$ photocatalyst. The polymerizations were performed using a molar ratio of $[monomers]_0/[MBP]_0/[Ir(ppy)]_0 = 100/1/2.5 \times 10^{-3}$ in ethanol. The reagents were degassed in the Schlenk tube before irradiation. At the end of the reaction, ethanol was removed by evaporation, and the resulting polymer was diluted in water and purified by dialysis against a 50/50 mixture of water/ethanol. The mechanism of the reaction is controlled by the photoactivation of the iridium catalyst to an excited state. The $Ir(ppy)_3$ catalyst absorbs light to produce a $Ir(ppy)_3$* high-energy state. The $Ir(ppy)_3$* excited state is able to react with the initiator of the polymerization, MBP, to produce the first radical, which starts the polymerization of the monomers. As a result, the iridium complex is converted to a higher oxidation state of Ir(IV). Subsequently, the ground-state $Ir(ppy)_3$ complex can be regenerated. The Ir(IV) complex can react with a propagating radical to regenerate the Ir(III) complex and the dormant species with a bromo end group. The cycle is restarted with the reaction of $Ir(ppy)_3$ and the dormant polymer chain to generate a new radical and the subsequent addition of a monomer [30, 38].

This photopolymerization method presents several advantages compared to ATRP-based methods. First, the reaction conditions used in the preparation of the polymers are relatively simple. Photopolymerization is performed at room temperature, and the iridium-based catalyst has low sensitivity to oxygen and water. The amount of catalyst used is very low (i.e., 25 ppm), and the catalyst is auto-

regenerated during the reaction in the presence of UV light. Moreover, reversible activation and deactivation of the polymerization is possible upon UV light irradiation. An added advantage of the iridium-based photopolymerization is the lack of exhaustive purification procedures required to remove the high amount of catalyst used in ATRP-based polymerization.

The P(MEO_2MA-co-$OEGMA_{500}$) polymers prepared by photopolymerization were analyzed by FTIR spectroscopy, ^1H NMR spectroscopy and GPC. The FTIR characterization of the P(MEO_2MA-co-$OEGMA_{500}$) polymer (Fig. 1a) shows a characteristic band at 2880 per cm attributed to C–H stretching vibrations. The peak at 1720 per cm is ascribed to the stretching vibrations of C=O groups in the polymer. The broad band at 1109 per cm corresponds to C–O–C stretching vibrations. The structure of P(MEO_2MA-co-$OEGMA_{500}$) was also confirmed by ^1H NMR analysis, as shown in Fig. 1b. Resonances are observed at 4.1 ppm (labeled as c: CH_2–CH_2–O), at 3.5–3.7 ppm (labeled as d) corresponding to methylenoxy –CH_2–O– protons of the repeating units, at 3.4 ppm (labeled as e) corresponding to methoxy –OCH_3 protons, at 1.7–2 ppm (a: –$CH_2C(CH_3)$), and at 0.7–1.1 ppm (b: –$CH_2C(CH_3)$). The signals in Fig. 1b confirmed that the P(MEO_2MA-co-$OEGMA_{500}$) copolymer was obtained.

The LCST of the polymer was set in the range of physiological temperatures to be potentially used in biomedical applications. The monomer ratio in the synthesis was adjusted to obtain a LCST of 43 °C. Figure 2 shows the transmittance curve of a 3 mg/ml polymer solution in water measured at 670 nm as a function of temperature. The [MEO_2MA]/[$OEGMA_{500}$] monomer molar ratio used as precursors in the synthesis was 88/12. The polymers obtained by photopolymerization presented a narrow phase transition, which is indicative of the precise control over the

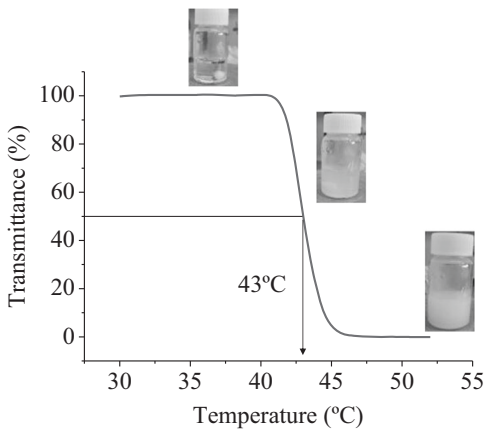

Fig. 2 Transmittance at 670 nm vs. temperature of a 3 mg/ml P(MEO_2MA-co-$OEGMA_{500}$) polymer solution. The LCST is 43 °C, and the MEO_2MA/$OEGMA_{500}$ ratio was set at 88:12 (Color figure online)

macromolecular structure rendering homogeneous chain-to-chain comonomer compositions [39]. The images in Fig. 2 represent the polymer solution behavior at different temperatures. Below the LCST, the solution is optically clear, as the polymer chains in solution are in an expanded coil conformation [39]. At the LCST, the polymer chains collapse and undergo a reversible coil-to-globule transition that can be observed directly by the turbidity of the polymer solution. The phase transition is reversible, as the interactions stabilizing these globular structures are ascribed to van der Waals forces [9].

The actual monomer ratio obtained in the polymer was calculated by ^1H NMR spectroscopy. The relative integrations of the peaks labeled "e" and "d" in Fig. 1b allowed to experimentally calculate the actual MEO_2MA/$OEGMA_{500}$ monomer content. Supplementary Fig. S2 (in the supporting information section) shows an example of the analysis to determine the actual monomer content present in the P(MEO_2MA-co-$OEGMA_{500}$) polymer. The average MEO_2MA/$OEGMA_{500}$ ratio obtained was $(89/11) \pm 0.5$. The standard deviation was determined from three independent syntheses. The ratio of MEO_2MA to $OEGMA_{500}$ calculated in the polymer was similar to the reagent feed ratio of MEO_2MA to $OEGMA_{500}$ (88/12).

A traditional ATRP synthetic method was tested and compared with the aforementioned photopolymerization. All the polymerizations were performed in ethanol using the same ratio of monomers to initiator, $[monomers]_0/[MBP]_0 = 100/1$. The feed molar ratio between monomers [MEO_2MA]/[$OEGMA_{500}$] was 88/12. The ATRPs were conducted at 60 °C; meanwhile, the photopolymerizations were conducted at room temperature. The amount of catalyst needed in ATRP was much higher than that in photopolymerization (Table 1). The polymerization kinetics were compared for the two synthesis methods. Monomer conversions over time were evaluated using ^1H NMR spectroscopy by comparing the integrated peak areas corresponding to the vinyl protons of the free monomers at

Table 1 Reaction conditions and monomer conversions of the thermoresponsive polymers prepared by the tested polymerization methods[a]

	T/°C	Catalyst/ppm[b]	Time/h	Conv/%[c]
Photopolymerization	rt	25	8	92.4 ± 5.1
ATRP	60	10,000	22	70.4 ± 3.6

[a]All polymerizations were conducted in ethanol and with $[monomers]_0/[initiator]_0=100/1$ (monomer/ethanol = 1/1.25 (v/v)). Feed monomer ratio [MEO_2MA]/[$OEGMA_{500}$] was 88/12

[b]Catalyst concentrations were calculated by the initial molar ratio of catalyst to the monomers

[c]Monomer conversions were determined by ^1H NMR spectroscopy. Reported values are means ± standard deviations of three independent syntheses

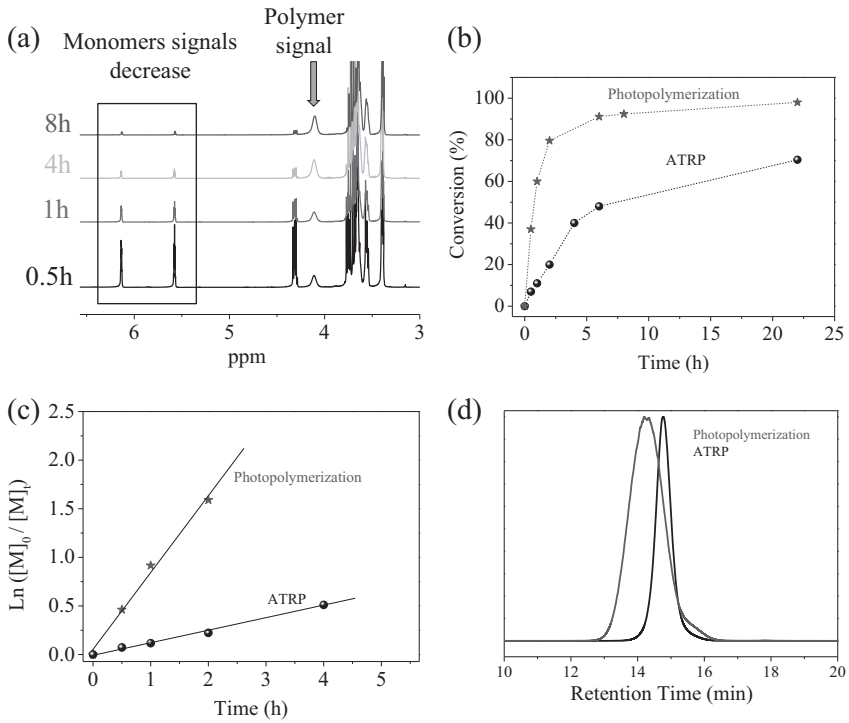

Fig. 3 **a** Evolution of the ^{1}H NMR spectrum with time during the photopolymerization reaction. **b** Monomer conversion determined by ^{1}H NMR spectroscopy. **c** Evolution of $\ln([M]_0/[M]_t)$ vs. reaction time, and **d** GPC chromatograms for P(MEO_2MA-co-$OEGMA_{500}$) prepared by photopolymerization and ATRP (Color figure online)

Table 2 Characterization of the thermoresponsive polymers prepared by the three evaluated polymerization methods[a]

	Mn_{GPC}/Da[b]	Mn_{th}/Da[c]	PDI_{GPC} (M_w/M_n)[b]
Photopolymerization	21334 ± 1885	20882	1.31 ± 0.03
ATRP	15210 ± 1147	15910	1.08 ± 0.0

[a]All polymerizations were conducted in ethanol and with $[monomers]_0/[initiator]_0 = 100/1$ (monomer/ethanol = 1/1.25 (v/v)). Feed monomer ratio $[MEO_2MA]/[OEGMA_{500}]$ was 88/12

[b]Measured by GPC calibrated against PMMA standards using THF as eluent. Reported values are means ± standard deviations of three independent syntheses

[c]The theoretical Mn was calculated as Mn_{th} = conversion (500 $[OEGMA]_0$ + 188 $[MEO_2MA]_0$)/$[Initiator]_0$

5.57 and 6.13 ppm to the integration of the spectral region (4.0–4.4 ppm), which corresponds to two protons of the free monomers and two protons of the polymer. These regions are highlighted in Fig. 3a. The results show the rapid evolution of the reaction in the case of the photopolymerization. In this case, the signals of the remaining monomers in the ^{1}H NMR spectrum decrease sharply over time, reaching >50% monomer conversion in less than 1 h of reaction. In Fig. 3b, the polymerization kinetic profiles showed that, in the photopolymerization, a final conversion greater than 90% was reached after only 6 h of reaction. In the case of ATRP, the final conversion obtained was ~70% after 22 h of reaction. Therefore, the photopolymerization is governed by a fast reaction rate, and a higher conversion is obtained when compared to the traditional Cu-based ATRP. The rate of reaction was evaluated by a plot of $\ln([M_0]/[M_t])$ vs. the reaction time, where M_0 and M_t represent the initial monomer concentration and the monomer concentration at a given time, respectively.

Figure 3c shows that the rate of polymerization was faster in photopolymerization than in ATRP; however, both reactions showed linear first-order kinetics. The polymerization rate is faster using photopolymerization compared to using traditional ATRP-based polymerization, as shown in Fig. 3c. In addition, the linear plot of $\ln([M_0]/[M_t])$ vs. reaction time suggested that constant concentrations of propagating free radicals were achieved during the polymerization [40], which is consistent with a controlled/living polymerization mechanism. To validate this behavior, the molecular weights and dispersities of the polymers obtained from the different polymerization reactions were analyzed (see Table 2).

Table 2 summarizes the properties of the polymers prepared in this study by photopolymerization and ATRP. The ATRP yielded the lowest dispersity of 1.08, however, the final conversion was lower (~70%) than that obtained using the photopolymerization. Typically, there is a gradual increase in dispersity with conversion [41]. Termination reactions that produce dead polymer chains occur during controlled radical polymerizations. At the beginning of the polymerization, the amount of dead chains generated by radical termination reactions is small, and thus, this factor has an insignificant contribution on the reduced dispersity. However, at high monomer conversion, the dead chain

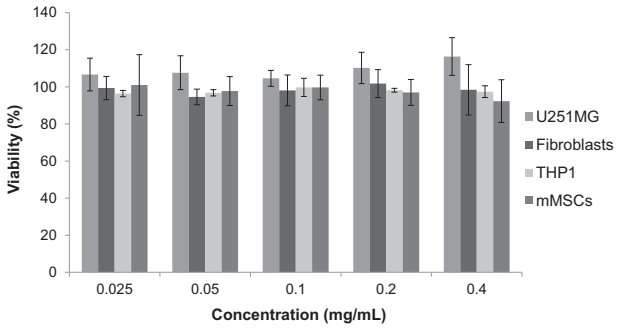

Fig. 4 Cell viability of the thermoresponsive polymer P(MEO_2MA-co-$OEGMA_{500}$) obtained by photopolymerization in four cell lines assayed after 24 h. Percentages are displayed as the mean ± standard deviations ($n = 5$) (Color figure online)

fraction increases, and its contribution to the dispersity increases with the conversion [42]. For instance, a sharp increase in dispersity has been observed for conversions above 90% in methyl methacrylate polymerization [43]. Additionally, Lutz et al. [15] demonstrated that the chloride-based ATRP catalyst used here gives excellent control over the polymerization of POEGMA with a molecular weight distribution close to 1 obtained at 83% conversion. However, when the monomer conversion was between 90–97%, the dispersity obtained for the copolymers increased to 1.22–1.72. Previous results of iridium-based photopolymerization of methyl methacrylate copolymers showed dispersity values of 1.24–1.36 [30], which are consistent with the dispersity values obtained in this work. Table 2 demonstrates that the photopolymerizations rendered a narrow final dispersity (close to 1.3), indicating the good control over the polymerization even at monomer conversions as high as 92%. Additionally, monomodal molecular weight distributions were observed by GPC (Fig. 3d). The theoretical Mn values were calculated from $Mn_{th} = \text{conversion} \ (500 \ [OEGMA]_0 + 188 \ [MEO_2MA]_0)/[\text{Initiator}]_0$. The Mn expected for 100% conversion in the synthesis was 22,600 Da. The theoretical molecular weight values presented in Table 2 obtained for the photopolymerized polymers were close to the experimental molecular weights obtained by GPC, which indicates that negligible termination reactions occurred during photopolymerization. The ATRP reactions also showed good agreement between the experimental and theoretical molecular weights. However, the ATRP-based polymerizations yielded lower molecular weights, which is consistent with the lower final conversion of the reaction (~70%) and low dispersity ($Mw/Mn = 1.08$).

In summary, the thermoresponsive polymer P(MEO_2MA-co-$OEGMA_{500}$) was successfully prepared by photopolymerization using the iridium-based catalyst Ir $(ppy)_3$ and MBP as initiator in ethanol under UV irradiation from two commercial LEDs. Photopolymerization provided good control over the molecular structure of the polymer. The experimental molecular weights were found to be close to the theoretical values, and the obtained dispersities were low (Mw/Mn ~1.3). The polymerization reaction rate (first-order kinetics) was fast and rendered a high monomer conversion.

To elucidate the in vitro cytotoxicity of the thermoresponsive polymer P(MEO_2MA-co-$OEGMA_{500}$) obtained by photopolymerization, its effects on cellular metabolism of four different mammalian cell lines were studied by the Blue Cell Viability assay at concentrations up to 0.4 mg/ml (Fig. 4). An increase in polymer concentration did not significantly decrease cell viability after 24 h, displaying percentages higher than 92% for all the cell types assayed. Accordingly, based on ISO 10993-5, which considers a reduction in cell viability higher than 30% as cytotoxic, our polymer showed high biocompatibility and suitability for biomedical applications.

Previous studies have also shown low cytotoxicities of different OEGMA-based copolymers prepared by ATRP on human hepatocarcinoma cells (HepG2) [44, 45], monkey kidney cells (COS-7) [46], and HeLa cells [47], exhibiting viability percentages in the same range as ours (>90%). However, these polymers were reported to be carefully purified, as their toxic polymerization residues can exert cytotoxic damage in cells [46], which does not occur in our photopolymerization synthesis, indicating its suitability in the fabrication of polymers intended for biomedical purposes. In a previous study, human H9 T cells showed high viability percentages (>80%) after treatment for 24 h with OEGMA-based copolymers (45 mg/ml) synthesized by ARGET ATRP using copper as a catalyst at an amount (25 ng/mg polymer) similar to ours (73 ng of Ir(ppy)3 per mg of monomers (OEGMA + MEO_2MA)). However, a hydrolysis byproduct, diethylene glycol monomethyl ether (DEGME), was found to be highly toxic [48]. Other polymers, such as poly(ethylene glycol) (PEG) with thiol-modified hyaluronan [49] or hyperbranched PEG-N-hydroxysuccinimide (HB-PEG-NHS) [50], have been used to synthesize thermoresponsive copolymers by "one-pot and one-step" deactivation-enhanced ATRP (DE-ATRP) method [49] and in situ DE-ATRP [50], respectively. Both studies highlighted the high viability (>80%) of 3T3 fibroblasts when treated for 48 h with their hydrogels at concentrations between 1 and 5 mg/ml, even in 3D cultures composed of rabbit or rat adipose-derived stem cells, which is in accordance with our data. Nanocomposite hydrogels based on POEGMA and rigid rod-like cellulose nanocrystals were assayed in 3T3 fibroblast cultures to study their effect on cell metabolism [51]. These studies did not show a significant decrease in cell viability compared to control samples, and POEGMA hydrogels containing cellulose

nanocrystals were able to support cell growth for 24 h. POEGMA copolymers synthesized by reversible addition-fragmentation chain transfer followed by Diels–Alder reaction and the self-assembly of POEGMA-b-POMFMA by nano-precipitation in aqueous solution involved the formation of micelles, which were successfully assayed in HeLa cells to display negligible cytotoxicity [52]. Therefore, the use of the P(MEO_2MA-co-$OEGMA_{500}$) polymer as a biomedical nanomaterial is highly recommended not only because of its clear biocompatibility, but also due to its thermoresponsive capacity, highlighting its potential as an efficient drug nanocarrier.

Conclusions

In this paper, the synthesis of thermoresponsive P(MEO_2MA-co-$OEGMA_{500}$) polymers was investigated using a novel photopolymerization procedure, which used an iridium-based catalyst $Ir(ppy)_3$. The results showed low dispersity and high control over the molecular weight and polymer composition using this photopolymerization method. Moreover, the photopolymerization achieved a high final conversion in a short time, and thus, the polymerization reaction rate is fast while maintaining excellent control over the polymer structure and architecture. A monomer conversion higher than 50% was achieved in less than 1 h of synthesis with a fast polymerization rate. The photocatalyzed reaction showed some advantages compared to classical ATRP. It is a user-friendly method with simple reaction conditions, as it was performed at room temperature, and the amount of catalyst used in the photopolymerization was much lower with a typical value of a few ppm of catalyst. Moreover, using this method, it was possible to reversibly activate and deactivate the polymerization upon UV light irradiation. In addition, the application of the thermoresponsive polymer synthesized by this novel polymerization methodology in the biomedical field was also supported by the high viability data obtained after incubation with different mammalian cell lines.

Acknowledgements We thank the ERC Consolidator Grant program (ERC-2013- CoG-614715, NANOHEDONISM) for the financial support. CIBER-BBN is an initiative funded by the VI National R&D&i Plan 2008–2011 financed by the Instituto de Salud Carlos III with the assistance of the European Regional Development Fund. We also acknowledge Dr Pilar Martin-Duque for gifting the U251 MG and mMSCs cell lines.

Compliance with ethical standards

Conflict of interest The authors declare that they have no competing interests.

References

1 Vancoillie G, Frank D, Hoogenboom R. Thermoresponsive poly(oligo ethylene glycol acrylates). Prog Polym Sci. 2014;39:1074–95.
2 García-Juan H, Nogales A, Blasco E, Martínez JC, Šics I, Ezquerra TA, Piñol M, Oriol L. Self-assembly of thermo and light responsive amphiphilic linear dendritic block copolymers. Eur Polym J. 2016;81:621–33.
3 Hu Z, Cai T, Chi C. Thermoresponsive oligo(ethylene glycol)-methacrylate- based polymers and microgels. Soft Matter. 2010;6:2115–23.
4 Timko BP, Arruebo M, Shankarappa SA, McAlvin JB, Okonkwo OS, Mizrahi B, Stefanescu CF, Gomez L, Zhu J, Zhu A, Santamaria J, Langer R, Kohane DS. Near-infrared–actuated devices for remotely controlled drug delivery. Proc Natl Acad Sci USA. 2014;111:1349–54.
5 Hemmer E, Quintanilla M, Légaré F, Vetrone F. Temperature-Induced energy transfer in dye-conjugated upconverting nanoparticles: a new candidate for nanothermometry. Chem Mater. 2015;27:235–44.
6 Schmidt S, Zeiser M, Hellweg T, Duschl C, Fery A, Möhwald H. Adhesion and mechanical properties of PNIPAM microgel films and their potential use as switchable cell culture substrates. Adv Funct Mater. 2010;20:3235–43.
7 Trongsatitkul T, Budhlall BM. Multicore–shell PNIPAm-co-PEGMa microcapsules for cell encapsulation. Langmuir. 2011;27:13468–80.
8 Ohya S, Nakayama Y, Matsuda T. Thermoresponsive artificial extracellular matrix for tissue engineering: hyaluronic acid bioconjugated with poly(N-isopropylacrylamide) grafts. Biomacromolecules. 2001;2:856–63.
9 Lutz J-F, Akdemir Ö, Hoth A. Point by point comparison of two thermosensitive polymers exhibiting a similar LCST: is the age of poly(NIPAM) over? J Am Chem Soc. 2006;128:13046–7.
10 Vihola H, Laukkanen A, Valtola L, Tenhu H, Hirvonen J. Cytotoxicity of thermosensitive polymers poly(N-isopropylacrylamide), poly(N-vinylcaprolactam) and amphiphilically modified poly(N-vinylcaprolactam). Biomaterials 2005;26:3055–64.
11 Cooperstein MA, Canavan HE. Assessment of cytotoxicity of (N-isopropyl acrylamide) and Poly(N-isopropyl acrylamide)-coated surfaces. Biointerphases. 2013;8:19.
12 Ward MA, Georgiou TK. Thermoresponsive terpolymers based on methacrylate monomers: effect of architecture and composition. J Polym Sci A Polym Chem. 2010;48:775–83.
13 Ward MA, Georgiou TK. Multicompartment thermoresponsive gels: does the length of the hydrophobic side group matter? Polym Chem. 2013;4:1893–902.
14 Ward MA, Georgiou TK. Thermoresponsive triblock copolymers based on methacrylate monomers: effect of molecular weight and composition. Soft Matter. 2012;8:2737–45.
15 Lutz J-F, Hoth A. Preparation of ideal PEG analogues with a tunable thermosensitivity by controlled radical copolymerization of 2-(2-methoxyethoxy)ethyl methacrylate and oligo(ethylene glycol) methacrylate. Macromolecules. 2006;39:893–6.
16 Wang XSF, Lascelles SA, Jackson R, Armes SP. Facile synthesis of well-defined water-soluble polymers via atom transfer radical polymerization in aqueous media at ambient temperature. Chem Commun. 1999;1817–8.
17 Coullerez G, Carlmark A, Malmström E, Jonsson M. Understanding copper-based atom-transfer radical polymerization in aqueous media. J Phys Chem A. 2004;108:7129–31.
18 Garnier S, Laschewsky A. Synthesis of new amphiphilic diblock copolymers and their self-assembly in aqueous solution. Macromolecules. 2005;38:7580–92.

19 Peng Z, Wang D, Liu X, Tong Z. RAFT synthesis of a water-soluble triblock copolymer of poly(styrenesulfonate)-b-poly(ethylene glycol)-b-poly(styrenesulfonate) using a macromolecular chain transfer agent in aqueous solution. J Polym Sci A Polym Chem. 2007;45:3698–706.
20 Keddie DJ, Moad G, Rizzardo E, Thang SH. RAFT agent design and synthesis. Macromolecules. 2012;45:5321–42.
21 Perrier S, Takolpuckdee P, Mars CA. Reversible addition−fragmentation chain transfer polymerization: end group modification for functionalized polymers and chain transfer agent recovery. Macromolecules. 2005;38:2033–6.
22 Boyer C, Whittaker MR, Luzon M, Davis TP. Design and synthesis of dual thermoresponsive and antifouling hybrid polymer/gold nanoparticles. Macromolecules. 2009;42:6917–26.
23 Matyjaszewski K, Xia J. Atom transfer radical polymerization. Chem Rev. 2001;101:2921–90.
24 Tsarevsky NV, Matyjaszewski K. "Green" atom transfer radical polymerization: from process design to preparation of well-defined environmentally friendly polymeric materials. Chem Rev. 2007;107:2270–99.
25 Ouchi M, Terashima T, Sawamoto M. Transition metal-catalyzed living radical polymerization: toward perfection in catalysis and precision polymer synthesis. Chem Rev. 2009;109:4963–5050.
26 Matyjaszewski K, Jakubowski W, Min K, Tang W, Huang J, Braunecker WA, Tsarevsky NV. Diminishing catalyst concentration in atom transfer radical polymerization with reducing agents. Proc Natl Acad Sci USA. 2006;103:15309–14.
27 Konkolewicz D, Magenau AJD, Averick SE, Simakova A, He H, Matyjaszewski K. ICAR ATRP with ppm Cu catalyst in water. Macromolecules. 2012;45:4461–8.
28 Anastasaki A, Willenbacher J, Fleischmann C, Gutekunst WR, Hawker CJ. End group modification of poly(acrylates) obtained via ATRP: a user guide. Polym Chem. 2017;8:689–97.
29 Matyjaszewski K, Wang J-L, Grimaud T, Shipp DA. Controlled/"living" atom transfer radical polymerization of methyl methacrylate using various initiation systems. Macromolecules. 1998;31:1527–34.
30 Fors BP, Hawker CJ. Control of a living radical polymerization of methacrylates by light. Angew Chem Int Ed. 2012;51:8850–3.
31 Treat NJ, Fors BP, Kramer JW, Christianson M, Chiu C-Y, Read de Alaniz J, Hawker CJ. Controlled radical polymerization of acrylates regulated by visible light. ACS Macro Lett. 2014;3:580–4.
32 Xu J, Atme A, Marques Martins AF, Jung K, Boyer C. Photoredox catalyst-mediated atom transfer radical addition for polymer functionalization under visible light. Polym Chem. 2014;5:3321–5.
33 Xu J, Jung K, Atme A, Shanmugam S, Boyer C. A robust and versatile photoinduced living polymerization of conjugated and unconjugated monomers and its oxygen tolerance. J Am Chem Soc. 2014;136:5508–19.
34 Ma W, Chen H, Ma Y, Zhao C, Yang W. Visible-light-induced controlled polymerization of hydrophilic monomers with Ir(ppy)3 as a photoredox catalyst in anisole. Macromol Chem Phys. 2014;215:1012–21.
35 Zhang X, Zhao C, Ma Y, Chen H, Yang W. One-pot synthesis of PTFEMA-b-PMMA-b-PTFEMA by controlled radical polymerization with a difunctional initiator in conjugation with photoredox catalyst of Ir(ppy)3 under visible light. Macromol Chem Phys. 2013;214:2624–31.
36 Adali-Kaya Z, Tse Sum Bui B, Falcimaigne-Cordin A, Haupt K. Molecularly imprinted polymer nanomaterials and nanocomposites: atom-transfer radical polymerization with acidic monomers. Angew Chem Int Ed. 2015;127:5281–4.
37 Aseyev V, Tenhu H, Winnik FM. Self organized nanostructures of amphiphilic block copolymers II. In: Axel HEM, Oleg B, editors. Berlin Heidelberg: Springer; 2010. p. 29–89.
38 Nguyen JD, Tucker JW, Konieczynska MD, Stephenson CRJ. Intermolecular atom transfer radical addition to olefins mediated by oxidative quenching of photoredox catalysts. J Am Chem Soc. 2011;133:4160–3.
39 Lutz J-F, Weichenhan K, Akdemir Ö, Hoth A. About the phase transitions in aqueous solutions of thermoresponsive copolymers and hydrogels based on 2-(2-methoxyethoxy)ethyl methacrylate and oligo(ethylene glycol) methacrylate. Macromolecules. 2007;40:2503–8.
40 Xu J, Shanmugam S, Duong HT, Boyer C. Organo-photocatalysts for photoinduced electron transfer-reversible addition-fragmentation chain transfer (PET-RAFT) polymerization. Polym Chem. 2015;6:5615–24.
41 Wang XS, Armes SP. Facile atom transfer radical polymerization of methoxy-capped oligo(ethylene glycol) methacrylate in aqueous media at ambient temperature. Macromolecules. 2000;33:6640–7.
42 Mastan E, Zhu S. A molecular weight distribution polydispersity equation for the ATRP system: quantifying the effect of radical termination. Macromolecules. 2015;48:6440–9.
43 Mohammad Rabea A, Zhu S. Controlled radical polymerization at high conversion: bulk ICAR ATRP of methyl methacrylate. Ind Eng Chem Res. 2014;53:3472–7.
44 Lutz J-F, Andrieu J, Üzgün S, Rudolph C, Agarwal S. Biocompatible, thermoresponsive, and biodegradable: simple preparation of "all-in-one" biorelevant polymers. Macromolecules. 2007;40:8540–3.
45 Deng L, Ren J, Li J, Leng J, Qu Y, Lin C, Shi D. Magnetothermally responsive star-block copolymeric micelles for controlled drug delivery and enhanced thermo-chemotherapy. Nanoscale. 2015;7:9655–63.
46 Lutz J-F, Andrieu J, Hoth A, Agarwal S. Synthesis of biorelevant polymers by controlled radical polymerization. Polym Prepr. 2008;49:312–3.
47 Lu B, Li L, Wei L, Guo X, Hou J, Liu Z. Synthesis and thermoresponsive self-assembly behavior of amphiphilic copolymer [small beta]-CD-(PCL-P(MEO2MA-co-PEGMA))21 for the controlled intracellular delivery of doxorubicin. RSC Adv. 2016;6:50993–1004.
48 Elias PZ, Liu GW, Wei H, Jensen MC, Horner PJ, Pun SH. A functionalized, injectable hydrogel for localized drug delivery with tunable thermosensitivity: synthesis and characterization of physical and toxicological properties. J Control Release. 2015;208:76–84.
49 Dong Y, Saeed AO, Hassan W, Keigher C, Zheng Y, Tai H, Pandit A, Wang W. "One-step" preparation of thiol-ene clickable PEG-based thermoresponsive hyperbranched copolymer for in situ crosslinking hybrid hydrogel. Macromol Rapid Commun. 2012;33:120–6.
50 A S, Xu Q, Zhou D, Gao Y, Vasquez JM, Greiser U, Wang W, Liu W, Wang W. Hyperbranched PEG-based multi-NHS polymer and bioconjugation with BSA. Polym Chem. 2017;8:1283–7.
51 De France KJ, Chan KJW, Cranston ED, Hoare T. Enhanced mechanical properties in cellulose nanocrystal–poly(oligoethylene glycol methacrylate) injectable nanocomposite hydrogels through control of physical and chemical cross-linking. Biomacromolecules. 2016;17:649–60.
52 Li H, Li J, Ke W, Ge Z. A near-infrared photothermal effect-responsive drug delivery system based on indocyanine green and doxorubicin-loaded polymeric micelles mediated by reversible Diels–Alder reaction. Macromol Rapid Commun. 2015;36:1841–9.